

Core scattering of Stark wave packets

M. L. Naudeau, C. I. Sukenik, and P. H. Bucksbaum

Physics Department, University of Michigan, Ann Arbor, Michigan 48109-1120

(Received 5 November 1996)

We investigate the wave-packet dynamics of electrons bound in the nonseparable potential of cesium in a static electric field using time-domain Ramsey interferometry. Specially shaped wave packets with low radial dispersion enable us to view the interaction between the wave packet and the atomic core. Experiments in cesium, together with quantum defect calculations of cesium and hydrogen, demonstrate changes in the motion and shape of these wave packets due to core scattering. [S1050-2947(97)07403-9]

PACS number(s): 32.80.Rm, 32.60.+i, 32.80.Qk

The dynamics of quantum systems whose classical counterparts are chaotic continues to be an active area of physics research. An important example is an atom in a static electric field. The classical hydrogen atom in an electric field is separable in parabolic coordinates and therefore the electron trajectories do not display chaotic behavior. For atoms other than hydrogen however, the motion of the valence electrons is nonseparable and may be chaotic. Alkali-metal atoms are particularly well suited for simple analysis because of the near-absence of multielectron effects: they consist of a single valence electron moving in a near-static potential, which is hydrogenic except near the ion core.

Alkali-metal atoms in strong electric fields (Stark atoms) have energy spectra that differ markedly from hydrogen. Hydrogen spectra show considerable regularity, and the eigenvalues between states of different principal quantum number can cross, forming degeneracies at specific values of the electric field. Alkali-metal Stark spectra show very low degeneracy, strong avoided crossings, and Wigner-like distributions of eigenvalue separations that have been related to the irregular motion of trajectories in the corresponding classical systems [1]. These avoided crossings in alkali-metal atoms are due to a coupling between parabolic states in the presence of the atomic core. The size or strength of an anticrossing is a function of the admixture of angular momenta of the states. States of high angular momentum character do not penetrate the atomic core and so are less likely to experience any coupling. If, however, the states have appreciable low angular momentum character, the anticrossings become quite large, resulting in a breakdown of the regular, hydrogenic spectra [2].

One approach to connecting the quantum eigenvalue spectrum to the classical picture of an orbiting electron is through closed-orbit theory [3]—an extension of the Gutzwiller trace formula. Spectra are not viewed at constant electric field, but rather using scaled coordinates and momenta [4]. The classical dynamics then depend not on the energy and field separately, but rather on the combination E/\sqrt{F} , where E is the energy of the state relative to the field-free ionization limit and F is the external field. (Atomic units are assumed throughout this paper.) The scaling is exact for hydrogen and approximate for alkali-metal atoms. The scaled spectra are then Fourier transformed to get a “recurrence spectrum,” which has peaks at scaled actions corresponding to classical orbits, which begin and end at the nucleus.

High-resolution scaled spectroscopy of bound states of lithium in a strong electric field showed that the recurrence spectrum has periodicities that are almost identical to hydrogen. The only striking differences in the recurrence spectra between lithium and hydrogen were some additional periodicities in lithium at actions corresponding to sums of different classical hydrogenic orbits [5]. These additional features were interpreted as quantum analogs of classical orbits that scatter into one another when the electron passes through the ion core.

Because we are interested in quantum dynamics, it seems natural to seek a method of viewing recurrence phenomena directly in the time domain. One approach is to trace the motion of spatially localized quantum superposition states, known as wave packets, as they orbit the atom and scatter from the core. Unfortunately, the connection between wave-packet dynamics and scaled energy spectroscopy is not simple because there is no easy way to produce a wave packet whose constituents all have the same scaled energy. Furthermore, highly localized wave packets disperse quickly [6]; despite periodic revivals, it is difficult to follow their motion over many orbits.

These difficulties impose some restrictions on experiments, yet for sufficiently short times the wave-packet–classical electron trajectory correspondence should be valid [7]. Furthermore, if the spread of constituent eigenstates is not too great, an average scaled energy for the system may be a useful concept. This paper presents high-resolution time-domain recurrence spectra for cesium wave packets in an electric field where the number of eigenstates excited has been deliberately limited. By comparing our results to quantum dynamics calculations, we can observe how the cesium Stark wave packets differ from their hydrogenic counterparts.

Alkali-metal Rydberg wave packets have been produced in Stark atoms before, and their short-term behavior for fields comparable to E_c was found to be similar to hydrogen [8]. These experiments were mostly conducted above the classical field ionization limit where the long-time behavior is dominated by a sequential decay of components of the wave packet due to field ionization [9]. To avoid this limitation, our work focuses on the region below E_c where the wave-packet amplitude does not decay due to field ionization.

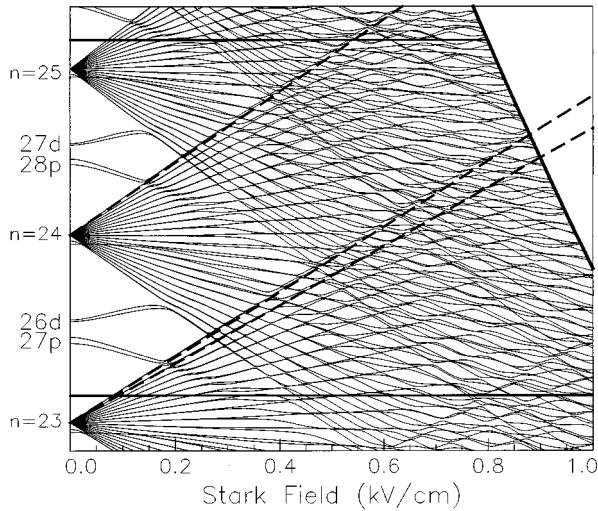


FIG. 1. Calculated Stark spectrum for cesium $|m_j|=1/2$. The classical field-ionization limit, $F_c = 1/16n^4$ is indicated by the bold curve. The shaped laser pulse excites eigenstates bounded by the two horizontal lines. Also shown are several hydrogenic levels (dashed lines). These give rise to the radial and angular return times $2\pi n^3$, and $2\pi/3nF$ as discussed in the text.

We use 100-fsec, 785-nm pulses from a Ti:sapphire laser employing Kerr-lens mode locking (KLM) and chirped-pulse amplification (CPA) [10]. This wavelength is centered on the transition between the $7s$ and $29p$ states in atomic cesium. In an electric field of several hundred volts per centimeter, the $7s$ state is nearly pure $l=0$, but the Rydberg l states are completely mixed. There is sufficient bandwidth in the short pulse to excite no fewer than 15 n states, which, including fine structure, contain more than 1000 discrete Stark energy eigenvalues producing a well-localized, and therefore highly dispersive wave packet.

The difficulty in charting the orbit of such a wave packet is that a coherent excitation with such a broad spread of energy-level spacings will quickly dephase, spreading the wave packet around the atom. This has been called wave-packet ‘‘collapse’’ [11]. To combat wave-packet collapse, we limit the number of states in the wave packet. This is done by shaping the frequency distribution of the exciting radiation pulse using spectral filters in the grating pulse expander and compressor, both of which are integral components of the CPA system [12]. The shaped pulse no longer has a Gaussian spectral distribution; rather the intensity is roughly constant over the bandwidth, although the frequency cutoff is not sharp. A good shape for our purpose is one that limits the radial dispersion by exciting only a few n manifolds of states, thus greatly simplifying the analysis of the wave-packet behavior.

Figure 1 shows the Stark states that are coherently excited by this shaped pulse. The initial states are produced in an atomic beam by two-photon excitation of the cesium $6s$ ground state to the $7s$ launch state using a 5-nsec, 1.08- μm laser pulse approximately 5 nsec prior to the wave-packet formation. The 1.08- μm light is generated in a hydrogen Raman cell, which shifts light from a Nd:YAG pumped pulsed dye laser. In our experiment, the polarization of the

100-fsec pulse is perpendicular to the applied electric field resulting in an initial excitation of both $|m_j|=1/2$ and $|m_j|=3/2$ states, which have some $l=1$ character. Fine structure must be included in our analysis as the spin-orbit interaction mixes $l=0$ states in the $|m_j|=1/2$ Stark manifold.

We have employed the technique of time-domain Ramsey interferometry [13]. Two wave packets are successively excited in the same atom by identical laser pulses separated by a variable time delay. The total excitation probability is the square of the sum of the amplitudes of the two packets. This is measured by field ionizing the Rydberg population of the atom and detecting the electrons with a microchannel electron multiplier. In the weak excitation limit, this signal is an autocorrelation function for the wave packet (analogous to a field autocorrelation function at the output of an optical interferometer).

The recurrence spectrum in the time domain is obtained by measuring the Rydberg population over several hundred picoseconds of delay. We then demodulate the high-frequency component, which arises from the optical quantum beat. Formally, this is a measurement of the autocorrelation function $|\langle \psi(t) | \psi(0) \rangle|$ [14]. A plot of the root-mean-square signal versus delay time between the two pulses shows peaks corresponding to times when the evolved wave packet most resembles its initial shape. The peaks recur on time scales that are characteristic of the energy spacings of the atom: $\delta\tau \sim 2\pi/\delta E$.

The Stark map in Fig. 1 shows the relevant time scales for the problem. The hydrogen-like splittings give rise to the two shortest times of interest: the so-called radial and angular motions of the wave packet. For $\bar{n}^* = 24$ (corresponding to an equal mixture of $27p$ and $28p$ in Cs), we have a radial period (or Kepler time) of $\tau_k = 2\pi\bar{n}^{*3} = 2.1$ psec. The electric field causes the orbital angular momentum to precess to a maximum value of $l \approx \bar{n}^* - 1 = 23$. For hydrogen, the precession time (parabolic orbit time, or angular return time) is $\tau_{\text{ang}} = 2\pi/3nF$, to first order in the electric field F . Judging from the irregularity of the Stark map, one would not expect to see distinguishable angular or radial returns in cesium. The only obvious time scale is that of the avoided crossings. The distribution of level splittings implies recurrences in the range ~ 50 – 200 psec.

Our experiments covered a range of τ_{ang} from 10 to 50 psec. The data are shown in the center column of Fig. 2. The interferograms show that the recurrences in cesium can be quite distinct, despite the irregular spectrum. The pure radial orbits can be seen in row (a). The laser spectrum is windowed so that only the $27p$ and $28p$ states are excited at zero field. The Kepler orbit time is 2.1 psec and the slow oscillation of approximately 60 psec is a quantum beat due to the spin-orbit interaction. The signal gradually decreases due to technical dephasing effects such as misalignment of the interferometer, inhomogeneities in the electric field, or Rydberg atom collisions. This decay places a limit of ~ 150 psec on our ability to monitor the wave-packet evolution.

In row (a), the electric field is nearly zero. A small drift field of 10 V/cm removes the electrons produced in multiphoton ionization from the 1.08- μm pump laser prior to wave-packet formation. This field strength has little effect on the cesium wave packet because of the quantum defect; however, in hydrogen, the p state is mixed into the manifold,

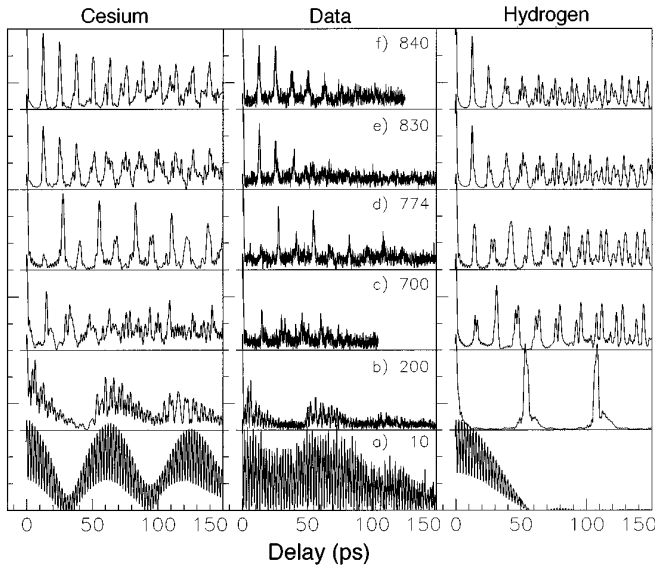


FIG. 2. Recurrence spectra for wave packets composed of Stark states indicated in Fig. 1. Left column: quantum defect theory calculation for cesium. Center column: experimental data. Right column: calculation for hydrogen. The static field was (a) 10 V/cm, (b) 200 V/cm, (c) 700 V/cm, (d) 774 V/cm, (e) 830 V/cm, and (f) 840 V/cm. Scales are identical for each plot. Curves are normalized to the coherent spike at zero delay time.

resulting in a very different wave-packet evolution than is observed at zero field. Only when the p state is well mixed with the rest of the manifold will the recurrence spectra for hydrogen and cesium begin to resemble each other (at around 300 V/cm).

Rows (b)–(f) of Fig. 2 show cesium interferograms at different Stark fields. The electric field produces a torque that causes the angular momentum of the wave packet to precess from its initial value of $l=1$ to higher angular momentum. When the evolved wave packet has predominantly high l character, the overlap with its initial state is small, resulting in a small signal. As the orbital angular momentum vector precesses back into its low values, the wave packet completes one parabolic orbit. The eigenstates have rephased to resemble the initial state and the overlap with the second pulse is large, resulting in a large signal. These cesium returns display certain characteristics that would be identified in hydrogen as a single angular return and radial returns resulting from the excitation of two p states. The times of these returns can be predicted by the hydrogenic formula discussed earlier. These features can also be reproduced in a quantum defect theory calculation (Fig. 2, left column) in which we approximate the frequency profile of our laser pulse to be a top hat.

It is instructive to compare our results with the predictions for a hydrogen atom excited under analogous conditions (same electric field and laser pulse). The results of the hydrogen calculation shown in Fig. 2, right column, are in strong disagreement with the data for cesium, even at high fields. This indicates that although the cesium data exhibit hydrogenlike properties, it is not appropriate to ignore the effects of the core.

The Stark state mixing in cesium makes it impossible to distinguish individual manifolds or even angular energy spacings within a manifold. In fact, the cesium interferograms suggest that what the system sees is an average effect. This results in a single, average radial return time and a single, average angular return time. The averaging effect also allows for interference between the angular and radial wave packets to an extent not seen in hydrogen.

The hydrogen wave function is a superposition of separate wave packets associated with different n manifolds (not the single manifold used to calculate the return times). Each n -manifold wave packet is parabolic, and therefore does not disperse; however, each manifold has a slightly different angular energy spacing, resulting in gradual dispersion of the wave packets from different manifolds. The peaks generally retain their shape as they separate, supporting the notion of a small number of essentially nondispersive wave packets being simultaneously excited. The core interaction in cesium prevents identifications of contributions from individual n manifolds. The wave packet excited in cesium contains many more frequencies “bunched” around a central value, and so the recurrences appear less dispersive.

Since the cesium wave packet does not disperse rapidly, we can follow the wave-packet trajectory over several classical orbits. When the field is small [row (b), $F=200$ V/cm for example], the parabolic precession is slow compared to the Kepler orbit time, so that the wave packet retains its p character over several Kepler cycles, resulting in very broad angular returns. At higher fields where the stronger torque causes the width of the angular recurrences to be on the order of the radial returns, peaks can be suppressed if the radial wave packet is at its outer turning point at the moment of an angular return. At $F=700$ V/cm, for example [row (c)], the second angular return occurred while the radial wave packet was at its outer turning point, resulting in a splitting of the peak. At a slightly higher field, $F=774$ V/cm, an individual angular return has been completely suppressed [row (d)]. This behavior is not possible in hydrogen because of the contributions from many different, noninteracting manifolds.

This effect can be exploited; by selecting a particular value of F , we can control the wave-packet behavior to enhance the interaction with the cesium core. For example, at $F=830$ V/cm, the radial and angular returns are nearly commensurate [row (e)]. This maximizes the core interaction with the wave packet, since each angular return coincides with a radial return spatially localized near the core.

Measurements of the time evolution of cesium Stark wave packets created below the classical field ionization threshold show remarkable regularity despite a very irregular eigenvalue spectrum. The irregular eigenvalue spectrum is a result of coupling between Stark states due to the presence of the large cesium core. The core blurs the contribution of individual manifolds and results in an averaging effect that gives the cesium wave-packet recurrence spectrum a more regular appearance than is the case for a hydrogen wave packet excited with the same bandwidth. In the language of classical phase space, this appearance of more regularity in the interferogram may be related to the destruction of some of the hydrogenic tori. The relationship between core scattering and

evolution of the wave packet may be quite useful in problems of quantum control of molecular dissociation or autoionization. It may also provide a useful comparison for classical trajectory models of complex quantum dynamics. These problems will be addressed in future work.

We wish to acknowledge many useful discussions with D. W. Schumacher, C. Raman, and C. W. S. Conover. This work was supported by the National Science Foundation. P.H.B. acknowledges partial support from the Miller Institute of the University of California at Berkeley.

-
- [1] M. Courtney, N. Spellmeyer, H. Jiao, and D. Kleppner, *Phys. Rev. A* **51**, 3604 (1995).
- [2] T. F. Gallagher, *Rydberg Atoms* (Cambridge University Press, Cambridge, 1994).
- [3] J. Gao and J. B. Delos, *Phys. Rev. A* **49**, 869 (1994).
- [4] U. Eichmann, K. Richter, D. Wintgen, and W. Sandner, *Phys. Rev. Lett.* **61**, 2438 (1988).
- [5] M. Courtney, H. Jiao, N. Spellmeyer, and D. Kleppner, *Phys. Rev. Lett.* **73**, 1340 (1994).
- [6] Z. D. Gaeta and C. R. Stroud, Jr., *Phys. Rev. A* **42**, 6308 (1990).
- [7] M. Mallalieu and C. R. Stroud, Jr., *Phys. Rev. A* **51**, 1827 (1995); Z. D. Gaeta, M. W. Noel, and C. R. Stroud, Jr., *Phys. Rev. Lett.* **73**, 636 (1994).
- [8] H. H. Fielding, J. Wals, W. J. van der Zande, and H. B. van Linden van den Heuvell, *Phys. Rev. A* **51**, 611 (1995); L. D. Noordam, A. Ten Wolde, A. Lagendijk, and H. B. van Lenden van den Heuvell, *ibid.* **40**, 6999 (1989); A. ten Wolde, L. D. Noordam, A. Lagendijk, and H. B. van Linden van den Heuvell, *Phys. Rev. Lett.* **61**, 2099 (1988).
- [9] B. Broers, J. F. Christian, and H. B. van Linden van den Heuvell, *Phys. Rev. A* **49**, 2498 (1994); B. Broers, J. F. Christian, J. H. Hoogenraad, W. J. van der Zande, H. B. van Lenden vanden Heuvell, and L. D. Noordam, *Phys. Rev. Lett.* **71**, 344 (1993); G. M. Lankhuijzen and L. D. Noordam, *Phys. Rev. A* **52**, 2016 (1995).
- [10] J. Squier, F. Salin, and G. Mourou, *Opt. Lett.* **16**, 324 (1991).
- [11] J. A. Yeazell, M. Mallalieu, and C. R. Stroud, Jr., *Phys. Rev. Lett.* **64**, 2007 (1990); J. Parker and C. R. Stroud, Jr., *ibid.* **56**, 716 (1986); G. Alber, H. Ritsch, and P. Zoller, *Phys. Rev. A* **34**, 1058 (1986).
- [12] A. M. Weiner, J. P. Heritage, and E. M. Kirschner, *J. Opt. Soc. Am. B* **5**, 1563 (1988).
- [13] L. D. Noordam, D. I. Duncan, and T. F. Gallagher, *Phys. Rev. A* **45**, 4734 (1992); J. F. Christian, B. Broers, J. H. Hoogenraad, W. J. van der Zande, and L. D. Noordam, *Opt. Commun.* **103**, 79 (1993).
- [14] M. Nauenberg, *J. Phys. B* **23**, L385 (1990).